

# Effect of Magnetic Field on the Electronic Transport in Trilayer Graphene

Yanping Liu,<sup>†</sup> Sarjoosing Goolaup,<sup>†</sup> Chandrasekhar Murapaka,<sup>†</sup> Wen Siang Lew,<sup>†,\*</sup> and Seng Kai Wong<sup>‡</sup>

<sup>†</sup>School of Physical and Mathematical Sciences, Nanyang Technological University, 21 Nanyang Link, Singapore 637371 and <sup>‡</sup>Data Storage Institute, (A\*STAR) Agency for Science, Technology and Research, DSI Building, 5 Engineering Drive 1, Singapore 117608

Graphene has generated tremendous interest owing to its novel electronic properties and unique energy band structure. The graphene energy–momentum relationship is found to be linear for low energies, leading to zero effective mass properties which can be described by the Dirac equation for spin  $1/2$  particles.<sup>1–5</sup> Graphene electrons and holes, referred to as Dirac fermions, are insensitive to external electrostatic potentials.<sup>6–8</sup> Because of the linear dispersion relation at low energies ( $E_F = \hbar v_F k$ ), one of the most interesting properties of graphene is that its low-energy excitations are massless, chiral Dirac fermions. In bilayer graphene, a parabolic band structure ( $E_F = \hbar^2 k^2 / 2m^*$ ) with an effective mass  $m^* = 0.037m_e$ , has been calculated with the interlayer coupling model.<sup>9–14</sup> Recent research has shown that bilayer graphene exhibits tunable bandgap under the application of a perpendicular electric field.<sup>15–18</sup> Graphene displays an unconventional Landau-level spectrum of mass chiral Dirac fermions with the presence of a magnetic field.<sup>3</sup> Recent research has shown that the energy splitting is proportional to  $\sqrt{B}$  for the symmetric case with half-filled zero-energy levels in both monolayer and bilayer graphene.

Trilayer graphene is very interesting as it has two almost linear conduction bands similar to monolayer graphene but also four parabolic bands, which is similar to bilayer graphene. For trilayer graphene, a similar dispersion relation as bilayer graphene with parabolic band structure, but with a larger effective mass  $m^* = 0.052m_e$ , has been found.<sup>19</sup> Zhu *et al.*,<sup>20</sup> have shown that the carrier density and mobility in bilayer and trilayer graphene display similar trends.

**ABSTRACT** The perpendicular magnetic field dependence of the longitudinal resistance in trilayer graphene at various temperatures has been systematically studied. For a fixed magnetic field, the trilayer graphene displays an intrinsic semiconductor behavior over the temperature range of 5–340 K. This is attributed to the parabolic band structure of trilayer graphene, where the Coulomb scattering is a strong function of temperature. The dependence of resistance on the magnetic field can be explained by the splitting of Landau levels (LLs). Our results reveal that the energy gap in the trilayer graphene is thermally activated and increases with  $\sqrt{B}$ .

**KEYWORDS:** trilayer graphene · electronic transport · coulomb scattering · magneto resistance · energy gap

Trilayer graphene has an intriguing band structure and the additional layers provide screening properties which cannot be obtained with mono- or bilayer graphene. Craciun *et al.* demonstrated that trilayer graphene is semimetallic with a tunable band gap overlap.<sup>19</sup> The electronic transport in trilayer graphene is dependent on various parameters. The experimental evidence of low energy electronic transport in graphene is not in agreement with the current theoretical model.<sup>21</sup> A better understanding on the general electronic transport properties of trilayer graphene is very important.

In this paper, we have carried out a systematic study on the charge transport properties in trilayer graphene as a function of magnetic field and temperature. We observed that the trilayer graphene exhibits an intrinsic semiconductor property even under the influence of an externally applied magnetic field. The resistance of the trilayer graphene decreases with increasing temperature and electric field; a behavior that is noticeably different from the experimental reports of monolayer graphene and bilayer graphene. The dependence of resistance on the magnetic field properties was observed. Our results reveal that the energy gap in the trilayer graphene is thermally

\*Address correspondence to wensiang@ntu.edu.sg.

Received for review June 9, 2010 and accepted October 28, 2010.

Published online November 3, 2010. 10.1021/nn101296x

© 2010 American Chemical Society

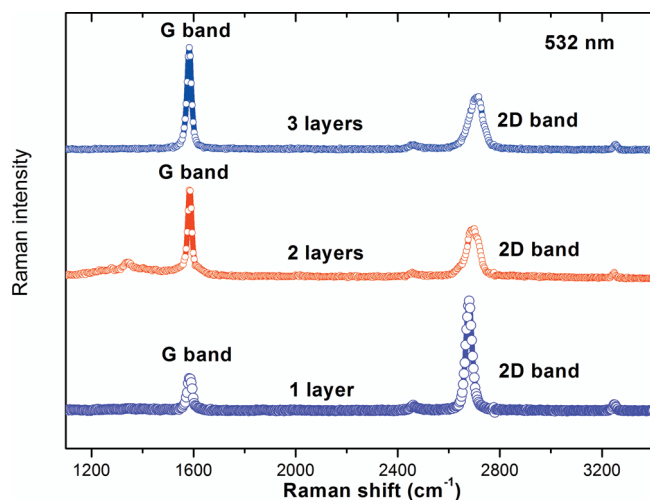


**Figure 1.** Comparison of Raman spectra at 532 nm for one- to three-layer graphene. The position of G peak and the spectral features of 2D band confirm the number of atomic layers of the graphene.

activated and increases with  $\sqrt{B}$ . This phenomenon originates from trilayer band structure that can be tuned by magnetic field, a property that has not been observed in other semimetal materials.

## RESULTS AND DISCUSSION

The precise number of graphene layers is identified using micro-Raman spectroscopy through the 2D-band deconvolution procedure.<sup>22–25</sup> The Raman spectra of our graphene structures were measured at room temperature using a WITEC CRM200 instrument at 532 nm excitation wavelength in the backscattering configuration.<sup>26–28</sup> Shown in Figure 1 is the characteristic Raman spectrum with a clearly distinguishable G peak and 2D band. The two most intense features are the G peak and the 2D band which is sensitive to the number of layers of graphene. The position of the G peak and the shape of the 2D band confirm the number of layers of graphene. The number of graphene layers can also be deduced from the full width half-maximum of the 2D band.

In Figure 2 we present the current–voltage characteristics of the trilayer graphene at temperatures,  $T$ , of 5 and 200 K, under the application of different magnetic fields. The magnetic field is applied perpendicular to the plane of the graphene. An optical image of the trilayer graphene is shown in the inset. For all our measurements, we observed a linear current–voltage ( $I$ / $V$ ) relationship, which is characteristic of ohmic behavior. The increase in resistance as the temperature is reduced is typical of an intrinsic semiconductor behavior.

However, for a fixed temperature, as the applied magnetic field increases, the resistance of the trilayer graphene increases. We attribute this to the perpendicular magnetic field opening an energy bandgap in the graphene structure.<sup>29–31</sup> Such behavior shows the opening energy gap by applied perpendicular magnetic field inducing high resistance. These observations suggest that the measured magnetic field dependence of the two-terminal longitudinal resistance  $R_{sd}$  for graphene is a qualitative fingerprint of the band gap.

To better understand the effect of perpendicular magnetic field on the electronic transport of trilayer graphene, we have carried out a systematic resistance measurement as a function of the magnetic field. Shown in Figure 3 is the two-terminal resistance,  $R_{sd}$  of trilayer graphene as a function of magnetic field at various temperatures. The term resistance per square is used as it is independent of the sample size. The resistance exhibits a nonlinear increase with the magnetic field. This arises from the spin splitting induced by the Zeeman effect. One of the unusual properties of massless Dirac electrons in graphene is that it has an intrinsic Zeeman energy equal to one-half of the cyclotron energy in a magnetic field. This results in Landau-level (LL) splitting of the energy levels into a spectrum comprising 12-fold degeneracy at zero-energy and 4-fold degeneracy at nonzero-energy levels in trilayer graphene.<sup>30,32</sup> This potentially indicates sublattice symmetry breaking and gap formation due to a many-body correction in the LL.<sup>33</sup> In addition, when Coulomb interaction is included, it gives rise to a gap opening at zero energy level due to the attractive interaction between electron–hole pairs forming an excitonic condensation. The gap ( $\Delta E_g$ ) is thermally activated and of excitonic nature and is proportional to  $\sqrt{B}$  according to

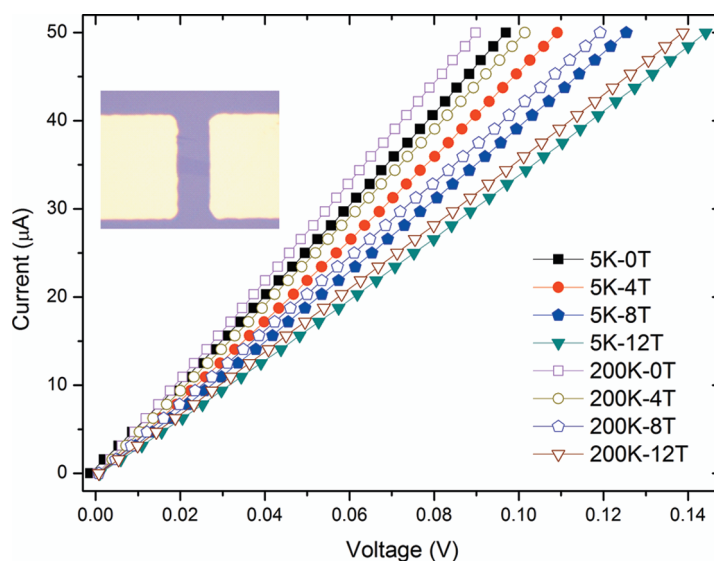


**Figure 2.** Temperature-dependent current–voltage characteristics of trilayer graphene. Inset shows the optical micrograph of the trilayer graphene with gold electrodes. The measurements show that trilayer graphene intrinsic semiconductor property and the introduction of a perpendicular magnetic field could induce high resistance.

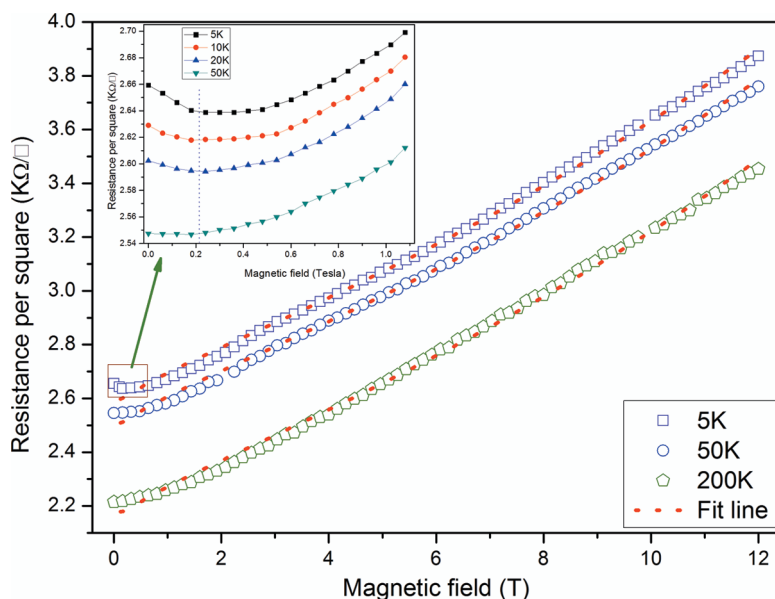


**Figure 3.** Resistance measurements as a function of temperature at temperature range of 5, 50, and 200 K. The results show that the resistance  $R_{sd}$  increases nonlinearly with the magnetic field strength. Inset shows the weak localization effect at low field measurements. The dotted line is fit following the report that this gap is of excitonic nature and will increase with  $\sqrt{B}$ .

the recent theoretical prediction.<sup>20,33</sup> On the other hand, for the nonzero energy level, the effective Coulomb potential depends on the spins and it results in valley polarization.<sup>34</sup>

In our measurements, we have found an approximate expression for the nonlinear resistance,  $R_{sd} \propto \exp(\sqrt{B}/(k_B T))$ , where  $k_B$  is the Boltzmann constant. Our experimental results fit well with this equation, as seen by the dotted line in Figure 3. However, comparing the results with that of monolayer graphene,<sup>35</sup> an apparent difference was the absence of a sharp increase in the resistance with the magnetic field and plateau-like phases. These considerations give qualitative explanation of the  $R_{sd}$  nonlinear behavior under the influence of a magnetic field. One should note that there is a plateau-like resistance for  $T < 50$  K at a low magnetic field. As seen from the inset, at low field, for  $T < 50$  K, a negative magnetoresistance is observed until a field of 0.2 T, followed by a plateau region in the trilayer graphene. This is a signature of the weak localization effect in graphene where the intervalley scattering dominates.<sup>35,36</sup>

The main scattering mechanisms in few layer graphene with massless Dirac-fermion (MDF) at low energies has been reported to be Coulomb scattering and short-range scattering.<sup>20</sup> The interplay between these two main scattering modes strongly affect the resistance of few layer graphene. The effect of temperature on the main scattering mechanisms of trilayer graphene is not yet established. To gain an insight into the dominant modes, we have carried out a systematic study of the resistance-temperature behavior in trilayer graphene.

In Figure 4a, we present the temperature dependence of the resistance of the trilayer graphene at a neutrality point, with an out of plane magnetic field of 12 T and without the applied magnetic field. As the temperature increases from 4 to 340 K, the resistance decreases, which confirms our previous observation that the trilayer graphene exhibits intrinsic semiconductor property. As the trilayer graphene has a predominantly parabolic band structure, the coulomb scattering is a strong function of temperature. The coulomb scattering varies inversely as the temperature; an increase in temperature leads to a decrease in coulomb scattering, hence a decrease in resistance.

The mobility of charge carriers in the trilayer graphene is dependent on the interplay between the two main scattering mechanisms, which in turn affects the resistance. On the basis of the Matthiessen's rule,<sup>20</sup> we can derive an approximation resistance equation:  $R_{\text{trilayer}} = R_{\text{C-trilayer}} + R_{\text{sr-trilayer}}$ , where  $R_{\text{C-trilayer}}$  and  $R_{\text{sr-trilayer}}$  are resistances arising from the Coulomb and short-range scatterings, respectively. We approximate the respective terms to be of the form  $R_{\text{C-trilayer}} = 1/((A + BT)ne)$ ,  $R_{\text{sr-trilayer}} = C$ , where  $A, B, C$  are the fitting parameters. We fitted our experimental results to the analytical expression and obtained the following:

$$R_{\text{trilayer}}(T, B = 0 \text{ T})/R_{\text{trilayer}}(T = 5 \text{ K}, B = 0 \text{ T}) = \frac{1}{0.68057 + 2.9711 \times 10^{-4}T} - 0.46831$$

$$R_{\text{trilayer}}(T, B = 12 \text{ T})/R_{\text{trilayer}}(T = 5 \text{ K}, B = 12 \text{ T}) = \frac{1}{0.11655 + 1.6439 \times 10^{-5}T} - 6.70767$$

From our experimental data fit, we note that the resis-

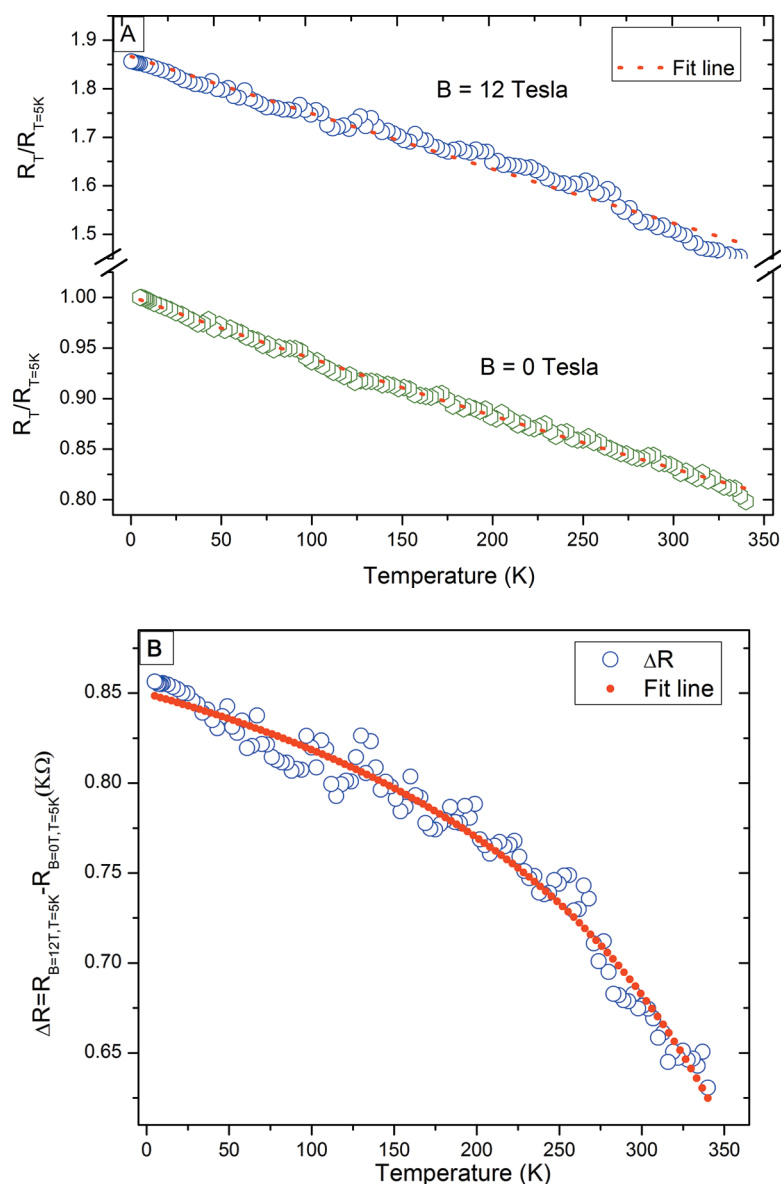


**Figure 4.** (A) Resistance measurements of trilayer graphene as a function of temperature at zero and 12 T magnetic fields. The symbols are the measured data and the lines are fits. The results show that the resistance of the trilayer graphene drops following a nonmetallic behavior. (B) The relative resistance change under the bias and unbiased magnetic field as a function of temperature, the line is the fit following the equation  $R_{sd} \propto \exp(\Delta E/(k_B T))$ .

tance component due to the short-range scattering is strongly influenced by the magnetic field. The short-range scattering arises from the potentials created by localized defects in the graphene structure. The application of a perpendicular magnetic field leads to a distortion of the graphene lattice. A detailed theoretical analysis of graphene in a magnetic field has shown that spontaneous lattice distortion lifts the valley degeneracy only in the lowest Landau level,  $n = 0$ , while the  $n > 0$  Landau levels remain a 2-fold valley degeneracy.<sup>35,37</sup> Figure 4b shows the relative change in resistance ( $\Delta R = R_{12T} - R_{0T}$ ) as a function of temperature.  $\Delta R$  displays a monotonic decrease as the temperature is increased. The dotted line is the fit to the equation  $R_{sd} \propto \exp(\Delta E/(k_B T))$ , where  $\Delta E$  is the energy gap. Our experimental results are in good agreement with

theory. These considerations give qualitative explanations to the decrease of the resistance with increasing temperature.

Figure 5 shows the measured normalized resistance of the trilayer graphene as a function of electric field  $E$ , under an applied magnetic field of 0–12 T and an operating temperature of 5–340 K. The measured  $R_{sd}-E$  plot is symmetrical with respect to the polarity  $E$  due to the chirality of graphene electrons when the applied electric field sweeps from  $+E$  to  $-E$ . For measurement at low electric field ( $E < 1$  mV/ $\mu\text{m}$ ), the results show that the resistance drops significantly when the magnetic field increases from 0 to 12 T at the lower temperature range of 5–50 K. The larger drop in the resistance at a lower temperature range ( $T < 50$  K) is due to the Coulomb impurities scattering which is a strong

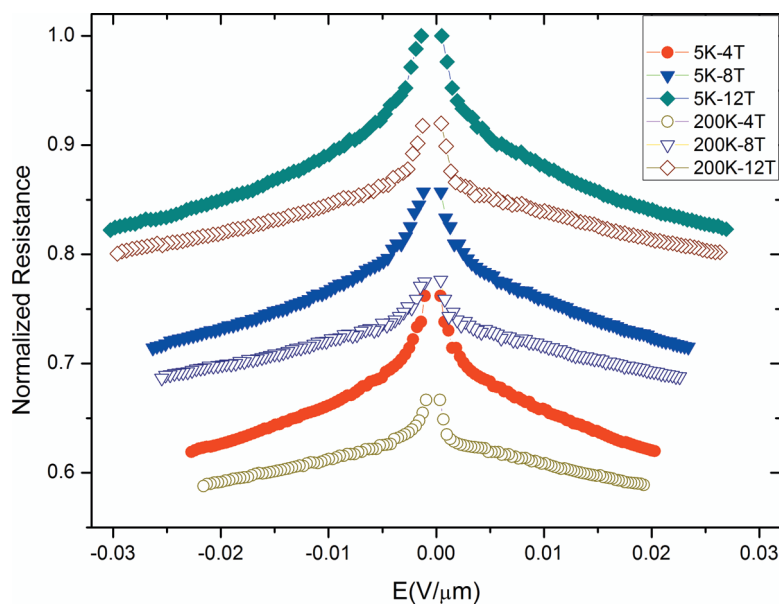


**Figure 5.** Electric and magnetic field dependent resistance measurements in trilayer graphene. The normalized resistance  $R$ – $E$  curve characteristic under the magnetic field from  $B = 0$  T to  $B = 12$  T and the temperature from 4 to 340 K, respectively. The results show that when the magnetic field increases from 0 to 12 T the resistance of the trilayer graphene rises significantly and it decreases with the increasing electric field.

function of temperature. On the other hand, for measurement at higher electric field ( $E > 10$  mV/ $\mu$ m), the overall resistance drops gradually as the temperature increases. The decrease is ascribed to the screening effect from the additional graphene layers on the scattering of thermally excited surface polar phonons of the SiO<sub>2</sub> substrate.<sup>38</sup> This result indicates that the scattering induced by electric field from the substrate surface polar phonons is significantly screened at high temperatures in trilayer graphene.

## CONCLUSIONS

The temperature and magnetic field dependence of the resistance of trilayer graphene has been investigated. Our results show that the resistance of trilayer graphene drops with increasing electric field, but in-

creases with magnetic field strength (0–12 T). The resistance dependence on temperature at a fixed magnetic field for trilayer graphene exhibits an intrinsic semiconductor nature. A model was formulated to explain the observed resistance dependence on the magnetic field and the measured normalized resistance as a function of temperature. The experimental results are in good agreement with theoretical prediction. Our results reveal that the energy gap in the trilayer graphene is thermally activated and increases with  $\sqrt{B}$ , which indicates sublattice symmetry breaking and gap formation due to a many-body correction in the Landau level. The obtained results are important for understanding that the resistance dependence on magnetic field is qualitative proof of an energy gap opening in trilayer graphene.

## METHODS

The graphene trilayer samples used in this work were fabricated using a method described in ref 2. Mechanical exfoliation of highly oriented pyrolytic graphite (grade ZYA, SPI Supplies) is used to deposit few-layer graphene flakes on a doped silicon substrate covered with a 300-nm thick layer thermally grown SiO<sub>2</sub>. The number of layers of trilayer graphene were identified by optical microscope and subsequently confirmed by Raman spectroscopy. The contact patterns were fabricated using photolithography techniques. A pair of ohmic Cr/Au (10 nm/90 nm) contacts was deposited *via* thermal evaporation at a background pressure of  $10^{-7}$  mbar and followed by a subsequent lift off in warm acetone. Electronic transport measurements were carried out in multiple samples, using PPMS (Quantum Design) with a fixed excitation current of 10  $\mu$ A. The measurements were performed in the temperature range 5–340 K, and a magnetic field up to 12 T was applied. To enhance the electrical transport, *in situ* magnetic and electric fields sample cleaning were carried out. We chose the two-probe technique for our trilayer

graphene transport measurement because it is relatively simple for electrode fabrication on graphene flakes and its reliability for graphene characterization has been confirmed by many researchers.<sup>19,29</sup>

**Acknowledgment.** This work was supported in part by the ASTAR SERC Grant (082 101 0015) and the NRF-CRP program (Multifunctional Spintronic Materials and Devices). We acknowledge F. T. Vasko (Institute of Semiconductor Physics) for useful discussions. We thank Cong Chunxiao for her supports in experimental measurements.

## REFERENCES AND NOTES

- Geim, A. K.; Novoselov, K. S. The Rise of Graphene. *Nat. Mater.* **2007**, *6*, 183–191.
- Novoselov, K. S.; Geim, A. K.; Morozov, S. V.; Jiang, D.; Zhang, Y.; Dubonos, S. V.; Grigorieva, I. V.; Firsov, A. A. Electric Field Effect in Atomically Thin Carbon Films. *Science* **2004**, *306*, 666–9.

3. Novoselov, K. S.; Geim, A. K.; Morozov, S. V.; Jiang, D.; Katsnelson, M. I.; Grigorieva, I. M.; Dubonos, S. V.; Firsov, A. A. Two-Dimensional Gas of Massless Dirac Fermions in Graphene. *Nature* **2005**, *438*, 197–200.
4. Novoselov, K. S.; Jiang, Z.; Zhang, Y.; Morozov, S. V.; Stormer, H. L.; Zeitler, U.; Maan, J. C.; Boebinger, G. S.; Kim, P.; Geim, A. K. Room-Temperature Quantum Hall Effect in Graphene. *Science* **2007**, *315*, 1379.
5. Wallace, P. R. The Band Theory of Graphite. *Phys. Rev.* **1947**, *71*, 622.
6. Semenoff, G. W. Condensed-Matter Simulation of a Three-Dimensional Anomaly. *Phys. Rev. Lett.* **1984**, *53*, 2449.
7. Geim, A. K. Graphene: Status and Prospects. *Science* **2009**, *324*, 1530–1534.
8. Kim, K. S.; Zhao, Y.; Jang, H.; Lee, S. Y.; Kim, J. M.; Ahn, J. H.; Kim, P.; Choi, J. Y.; Hong, B. H. Large-Scale Pattern Growth of Graphene Films for Stretchable Transparent Electrodes. *Nature* **2009**, *457*, 706–710.
9. Shen, T.; Gu, J. J.; Xu, M.; Wu, Y. Q.; Bolen, M. L.; Capano, M. A.; Engel, L. W.; Ye, P. D. Observation of Quantum-Hall Effect in Gated Epitaxial Graphene Grown on SiC (0001). *Appl. Phys. Lett.* **2009**, *95*, 172105.
10. Wu, X. S.; Hu, Y. K.; Ruan, M.; Madiomanana, N. K.; Hankinson, J.; Sprinkle, M.; Berger, C.; de Heer, W. A. Half Integer Quantum Hall Effect in High Mobility Single Layer Epitaxial Graphene. *Appl. Phys. Lett.* **2009**, *95*, 223108.
11. Meyer, J. C.; Geim, A. K.; Katsnelson, M. I.; Novoselov, K. S.; Booth, T. J.; Roth, S. The Structure of Suspended Graphene Sheets. *Nature* **2007**, *446*, 60–3.
12. Barone, V.; Hod, O.; Scuseria, G. E. Electronic Structure and Stability of Semiconducting Graphene Nanoribbons. *Nano Lett.* **2006**, *6*, 2748–2754.
13. Han, M. Y.; Ozyilmaz, B.; Zhang, Y. B.; Kim, P. Energy Band-Gap Engineering of Graphene Nanoribbons. *Phys. Rev. Lett.* **2007**, *98*, 206805.
14. Wang, Z. F.; Shi, Q. W.; Li, Q. X.; Wang, X. P.; Hou, J. G.; Zheng, H. X.; Yao, Y.; Chen, J. Z-Shaped Graphene Nanoribbon Quantum Dot Device. *Appl. Phys. Lett.* **2007**, *91*, 053109.
15. Zhang, Y.; Tang, T.-T.; Girit, C.; Hao, Z.; Martin, M. C.; Zettl, A.; Crommie, M. F.; Shen, Y. R.; Wang, F. Direct Observation of a Widely Tunable Bandgap in Bilayer Graphene. *Nature* **2009**, *459*, 820–823.
16. Kuzmenko, A. B.; Crassee, I.; van der Marel, D.; Blake, P.; Novoselov, K. S. Determination of the Gate-tunable Band Gap and Tight-Binding Parameters in Bilayer Graphene Using Infrared Spectroscopy. *Phys. Rev. B* **2009**, *80*, 165406.
17. Morozov, S. V.; Novoselov, K. S.; Katsnelson, M. I.; Schedin, F.; Elias, D. C.; Jaszczak, J. A.; Geim, A. K. Giant Intrinsic Carrier Mobilities in Graphene and Its Bilayer. *Phys. Rev. Lett.* **2008**, *100*, 016602.
18. Bisti, V. E.; Kirova, N. N. Charge Density Excitations in Bilayer Graphene in High Magnetic Field. *J. Exp. Theor. Phys. Lett.* **2009**, *90*, 120–123.
19. Craciun, M. F.; Russo, S.; Yamamoto, M.; Oostinga, J. B.; Morpurgo, A. F.; Tarucha, S. Trilayer Graphene Is a Semimetal with a Gate-Tunable Band Overlap. *Nat. Nano* **2009**, *4*, 383–388.
20. Zhu, W.; Perebeinos, V.; Freitag, M.; Avouris, P. Carrier Scattering, Mobilities, and Electrostatic Potential in Monolayer, Bilayer, and Trilayer Graphene. *Phys. Rev. B* **2009**, *80*, 235402.
21. Neto, A. H. C.; Guinea, F.; Peres, N. M. R.; Novoselov, K. S.; Geim, A. K. The Electronic Properties of Graphene. *Rev. Mod. Phys.* **2009**, *81*, 109–62.
22. Malard, L. M.; Pimenta, M. A.; Dresselhaus, G.; Dresselhaus, M. S. Raman Spectroscopy in Graphene. *Phys. Rep.* **2009**, *473*, 51–87.
23. Calizo, I.; Bejenari, I.; Rahman, M.; Guanxiong, L.; Balandin, A. A. Ultraviolet Raman Microscopy of Single and Multilayer Graphene. *J. Appl. Phys.* **2009**, *106*, 043509.
24. Hao, Y. F.; Wang, Y. Y.; Wang, L.; Ni, Z. H.; Wang, Z. Q.; Wang, R.; Koo, C. K.; Shen, Z. X.; Thong, J. T. L. Probing Layer Number and Stacking Order of Few-Layer Graphene by Raman Spectroscopy. *Small* **2010**, *6*, 195–200.
25. Ni, Z. H.; Wang, Y. Y.; Yu, T.; Shen, Z. X. Raman Spectroscopy and Imaging of Graphene. *Nano Res.* **2008**, *1*, 273–291.
26. Ferrari, A. C.; Meyer, J. C.; Scardaci, V.; Casiraghi, C.; Lazzeri, M.; Mauri, F.; Piscanec, S.; Jiang, D.; Novoselov, K. S.; Roth, S.; Geim, A. K. Raman Spectrum of Graphene and Graphene Layers. *Phys. Rev. Lett.* **2006**, *97*, 187401.
27. Ni, Z. H.; Wang, H. M.; Kasim, J.; Feng, H. Y. P.; Shen, Z. X. Graphene Thickness Determination Using Reflection and Contrast Spectroscopy. *Nano Lett.* **2007**, *7*, 2758–63.
28. Xuefeng, W.; Ming, Z.; Nolte, D. D. Optical Contrast and Clarity of Graphene on an Arbitrary Substrate. *Appl. Phys. Lett.* **2009**, *95*, 081102.
29. Krstici, V.; Oberfell, D.; Hansel, S.; Rikken, G. L. J. A.; Blokland, J. H.; Ferreira, M. S.; Roth, S. Graphene-Metal Interface: Two-Terminal Resistance of Low-Mobility Graphene in High Magnetic Fields. *Nano Lett.* **2008**, *8*, 1700–1703.
30. Barlas, Y.; Cote, R.; Nomura, K.; MacDonald, A. H. Intra-Landau-Level Cyclotron Resonance in Bilayer Graphene. *Phys. Rev. Lett.* **2008**, *101*, 097601.
31. Giesbers, A. J. M.; Ponomarenko, L. A.; Novoselov, K. S.; Geim, A. K.; Katsnelson, M. I.; Maan, J. C.; Zeitler, U. Gap Opening in the Zeroth Landau Level of Graphene. *Phys. Rev. B* **2009**, *80*, 201403.
32. Zhang, Y.; Jiang, Z.; Small, J. P.; Purewal, M. S.; Tan, Y. W.; Fazlollahi, M.; Chudow, J. D.; Jaszczak, J. A.; Stormer, H. L.; Kim, P. Landau-Level Splitting in Graphene in High Magnetic Fields. *Phys. Rev. Lett.* **2006**, *96*, 136806.
33. Khveshchenko, D. V. Magnetic-Field-Induced Insulating Behavior in Highly Oriented Pyrolytic Graphite. *Phys. Rev. Lett.* **2001**, *87*, 206401.
34. Ezawa, M. Intrinsic Zeeman Effect in Graphene. *J. Phys. Soc. Jpn.* **2007**, *76*, 094701.
35. Abergel, D. S. L.; Apalkov, V.; Berashevich, J.; Ziegler, K.; Chakraborty, T. Properties of Graphene: A Theoretical Perspective. *Adv. Phys.* **2010**, *59*, 261–482.
36. Ki, D. K.; Jeong, D.; Choi, J. H.; Lee, H.-J.; Park, K. S. Inelastic Scattering in a Monolayer Graphene Sheet: A Weak-Localization Study. *Phys. Rev. B* **2008**, *78*, 125409.
37. Apalkov, V. M.; Chakraborty, T. Fractional Quantum Hall States of Dirac Electrons in Graphene. *Phys. Rev. Lett.* **2006**, *97*, 126801.
38. Guinea, F. Charge Distribution and Screening in Layered Graphene Systems. *Phys. Rev. B* **2007**, *75*, 235433.